Quantum mechanical analysis of decomposition pathways of chloromethyl hypochlorite

Filothei Anagnostou, Evangelos Drougas, Agnie M. Kosmas*

Physical Chemistry Laboratory, Department of Chemistry, University of Ioannina, 451 10 Ioannina, Greece

Abstract

The most important decomposition pathways of chloromethyl hypochlorite, ClCH$_2$OCl, are examined using molecular structure quantum mechanical techniques. Specifically, the 1,1 and 1,2 elimination reactions, the isomerization channel and the C–O, O–Cl bond scissions are considered. The theoretical investigation yields high barriers for all production channels, which emphasize the high stability of ClCH$_2$OCl. Among the various reaction pathways, only the 1,2 eliminations to CH$_2$O + Cl$_2$ and ClCHO + HCl and the isomerization to dichloromethanol lead to more stable species. The photolytic O–Cl bond scission presents the lowest critical energy for reaction at the CCSD(T) level. Comparison with literature reports about the decomposition scheme of simple methyl hypochlorite, CH$_3$OCl, and fluoromethyl hypochlorite, FCH$_2$OCl, indicates a moderate effect of the different substitute on the dissociation pattern of these compounds.
© 2005 Elsevier B.V. All rights reserved.

Keywords: Chloromethyl hypochlorite; Elimination; Isomerization; Bond scission

1. Introduction

Plain and halogenated alkyl hypohalites have been interesting atmospheric species, ever since the first observation of the severe depletion of stratospheric ozone by chlorine derivatives [1]. They are formed from alkyl and halogenated alkyl radicals produced in the photofragmentation of halocarbons and play a significant role in the mechanism of the degradation processes of organic materials in the atmosphere and in various combustion systems. The insertion of an halogen in the methyl group lowers the reactivity towards O$_2$ and allows readily the haloalkyl radicals to build up to significant concentrations that are known to react with various radicals like OH, HO$_2$ and ClO. The association reactions with chlorine monoxide in particular, lead to chemically activated hypochlorites, which can either be stabilized and give temporary chlorine reservoirs or dissociate into lower energy products. Hence, much interest has been attached to these compounds and several theoretical and experimental investigations have

been carried out to examine their structure and reactivity [2–17]. Quantum mechanical calculations of CH$_3$OCl have shown that the most probable kinetically decomposition pathways, the 1,2 elimination to HCHO + HCl and the isomerization to chloromethanol [11,14], present high barriers, which demonstrate the considerable stability of the compound. Jung et al. [12] have made a comparative investigation of various hypochlorites and they have found severe stabilization of the resulting hypochlorite upon successive chlorination of the methylic group. Indeed, their enthalpy of formation calculations have shown that ΔH_f^{298} of CH$_2$ClOCl is lower by about 7 kcal mol^{-1} compared to the non-substituted analogue, CH$_3$OCl.

In view of these findings, it is also interesting to examine the dissociation of chloromethyl hypochlorite and the extent to which the substitution of a methylic hydrogen by a chlorine atom may affect the decomposition scheme. Thus, in the present work we employ molecular electronic structure calculations to study the various decomposition channels of ClCH$_2$OCl and determine the most probable reaction pathways. A detailed comparison is made with the decomposition scheme of plain methyl hypochlorite, CH$_3$OCl [11,14], and fluoromethyl hypochlorite, FCH$_2$OCl [17], to probe possible effects of the different substitutes on the stability of these compounds.

---

* Corresponding author. Tel.: +30 26510 98441; fax: +30 26510 98798.
E-mail address: amylona@cc.uoi.gr (A.M. Kosmas).

2. Computational details

The following channels have been considered in the decomposition scheme:

$$ClCH_2OCl \rightarrow TS1 \rightarrow HCOCl$$

$$+ HCl \quad (1, 1 \text{ elimination}) \tag{1}$$

$$\rightarrow TS2 \rightarrow ClCOCl + H_2 \quad (1, 1 \text{ elimination}) \tag{2}$$

$$\rightarrow TS3 \rightarrow HCClO + HCl \quad (1, 2 \text{ elimination}) \tag{3}$$

$$\rightarrow TS4 \rightarrow HCHO + Cl_2 \quad (1, 2 \text{ elimination}) \tag{4}$$

$$\rightarrow TSi \rightarrow Cl_2CHOH \quad (\text{isomerization}) \tag{5}$$
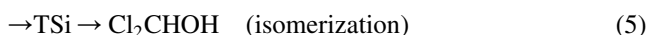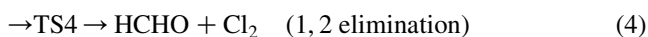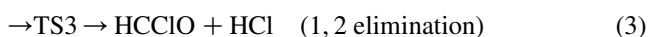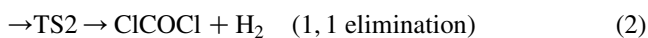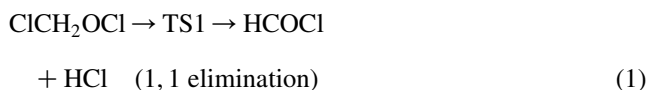
The photolytic Cl release through O–Cl bond breaking

$$ClCH_2OCl \rightarrow ClCH_2O + Cl \tag{6}$$

and the association reaction or the reverse C–O bond scission channel

$$ClCH_2 + OCl \leftrightarrow ClCH_2OCl \tag{7}$$
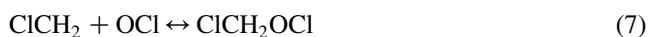
have also been examined.

The optimization of the various species involved in the dissociation scheme has been carried out at the B3LYP/6-311+G(d,p) and MP2/6-311+G(d,p) levels of theory. No symmetry constraints have been imposed and the potential energy surface has the A′ asymptote. Harmonic vibrational frequencies were computed at the same levels to characterize the stationary points and transition states were identified by one imaginary frequency as first order saddle points. The energetics were further refined using the G2MP2 method and by performing single-point CCSD(T)/6-311+G(d,p) calculations at the MP2/6-311+G(d,p) optimized geometries.

All computations have been carried out using the GAUSSIAN 98 series of programs [18].

3. Results and discussion

The geometrical and harmonic frequency results are summarized in Tables 1–4 while Figs. 1 and 2 contain the conformeric and isomeric structures of ClCH₂OCl and the transition state geometries, respectively. Table 5 includes the relative energy results and Figs. 3 and 4 present the energy profile of the dissociation scheme at the G2MP2 and CCSD(T) levels of theory, respectively. The optimized structures of reactants and products obtained using both methods, B3LYP/6-311+G(d,p) and MP2/6-311+G (d,p), are fully consistent with each

Table 1

Structural parameters (Å, deg) of reactants and products involved in ClCH₂OCl decomposition at the B3LYP/6-311+G (d,p) (first line) and MP2/6-311+G (d,p) (second line) levels of theory

Species	ClCH₂OCl	Cl₂CHOH	*cis*-HCOCl	*cis*-ClCOCl	ClCHO	ClCH₂O
r (O–Cl)	1.742, 1.739[a]		2.333	2.282		
	1.721		2.276	2.292		
r (O–H)		0.967				
		0.965				
r (C–O)	1.388, 1.390	1.354	1.148	1.166	1.179	1.348
	1.396	1.365	1.168	1.178	1.178	1.340
r (C–Cl)	1.817, 1.818	1.821		1.671	1.796	1.816
	1.779	1.785		1.665	1.763	1.793
r (C–H)	1.090, 1.091	1.083	1.096		1.096	1.097
	1.090	1.085	1.098		1.096	1.097
<) COCl	113.0, 113.1		116.9	118.7		
	111.5		119.3	120.0		
<) ClCO	113.9, 114.1	112.4		135.7	123.4	116.0
	113.5	112.1		134.3	123.6	115.4
<) HCO	113.1, 112.1	110.4	137.3		127.0	108.6
	111.9	108.6	135.3		126.2	108.5
<) H′CO	104.0, 103.9					
	103.7					
<) ClCH	106.6	106.9			109.5	108.1
	107.5	107.6			110.2	107.8
<) HCH′	112.4, 112.4					
	112.1					
φ(ClCOCl)	74.7, 74.7					
	72.6					
φ(ClCOH)		61.7				
		61.9				

[a] Results of Ref. 12.

Table 2
Important changes in the structural parameters (Å, deg) of $ClCH_2OCl$ conformers at the B3LYP/6-311+G (d,p) (first line) and MP2/6-311+G (d,p) (second line) levels of theory

Species	r(O–Cl)	r(C–O)	r(Cl–C)	<)ClCO	<)COCl	<)ClCOCl	<)HCOCl
$ClCH_2OCl$	1.742	1.388	1.817	113.9	113.0	74.7	47.2
	1.721	1.396	1.779	113.5	111.5	72.6	49.3
C_1	1.745	1.421	1.782	104.5	109.3	180.0	63.0
	1.721	1.420	1.752	105.2	108.2	180.0	62.0
C_2	1.738	1.405	1.815	110.0	113.6	117.7	0.0
	1.717	1.411	1.775	109.7	112.5	118.7	0.0
C_3	1.723	1.436	1.788	117.9	119.7	0.0	119.8
	1.708	1.436	1.760	117.8	118.9	0.0	120.6

other and also in good agreement with the results of Jung et al. [12]. Few discrepancies between the two methods are observed in the transition state configurations, which will be discussed in the detailed description of the decomposition pathways.

3.1. Energy minima

Chloromethyl hypochlorite presents four conformeric structures. The global minimum in the conformational potential energy surface, denoted hereafter as C_0, is characterized by C_1 symmetry with the hypochlorite chlorine located *gauch* to both the methylic chlorine and one methylic hydrogen. This geometry is the result

of the better interaction of the lone pair electrons on O with the non-occupied σ* (Cl–C) molecular orbital, thus, leading to a minimization of the energy [15]. In addition, the distance between the nearest methylic hydrogen and the hypochlorite chlorine, ∼2.28 Å, is in the range of distances that favour significant H–Cl interactions and contribute to the energy minimization. The comparison of the structural parameters between plain [11,14] and fluorinated hypochlorite [17] is interesting. The effect of chlorine α-substitution on the molecular geometry is shown in the shortening of the C–O bond (1.429 Å in CH_3OCl to 1.396 Å in $ClCH_2OCl$ at the MP2 level) and the slight elongation of the O–Cl bond (1.716 Å in CH_3OCl to 1.721 Å in $ClCH_2OCl$ at the same level),

Table 3
Structural parameters (Å, deg) of transition states involved in $ClCH_2OCl$ decomposition at the B3LYP/6-311+G (d,p) (first line) and MP2/6-311+G (d,p) (second line) levels of theory

Species	TS1	TS2	TS3	TS4	TSi
r (O–Cl)	2.045	2.248	2.422	2.369	2.206
	2.190	2.201	2.390	2.706	2.081
r (O–H)					1.159
					1.148
r (C–O)	1.214	1.204	1.265	1.232	1.326
	1.210	1.213	1.273	1.301	1.362
r (C–Cl)	2.516	1.721	1.816	2.293	1.714
	2.175	1.708	1.788	1.809	1.704
r (C–H)	1.090	1.502	1.203	1.093	1.089
	1.089	1.501	1.204	1.100	1.091
r (C–H)	1.179	1.228	1.104	1.103	1.383
	1.177	1.233	1.103	1.113	1.347
<) COCl	117.7	115.4	91.8	102.2	116.5
	114.3	115.7	90.8	90.6	119.9
<) ClCO	121.2	130.2	120.0	100.3	120.2
	118.4	128.4	119.1	108.9	118.5
<) HCO	125.7	117.0	99.9	118.3	120.3
	128.0	118.5	101.2	117.9	118.4
<) H'CO	117.4	111.1	118.1	122.5	50.6
	114.0	112.9	117.8	112.3	50.1
<) ClCH	96.6	100.6	102.5	86.0	114.3
	99.6	99.7	103.2	104.4	114.3
<) HCH'	116.4	37.5	103.4	116.3	109.8
	117.2	38.7	102.3	104.0	110.8
ClCOCl	109.6	56.7	103.7	46.2	77.1
	90.0	53.9	101.6	47.8	75.1

Table 4
Unscaled vibrational frequencies (cm^{-1}) of reactants and transition states involved in ClCH$_2$OCl decomposition at the B3LYP/6-311+G (d,p) (first line) and MP2/6-311+G (d,p) (second line) levels of theory

Species	
ClCH$_2$OCl	123, 319, 444, 631, 689, 978, 1043, 1262, 1341, 1453, 3080, 3156
	133, 326, 465, 665, 774, 1027, 1080, 1299, 1404, 1477, 3134, 3220
	124, 321, 448, 651, 692, 987, 1063, 1265, 1347, 1465, 3091, 3171[a]
Cl$_2$CHOH	274, 315, 447, 466, 660, 694, 1135, 1243, 1255, 1406, 3185, 3781
	296, 335, 469, 478, 716, 799, 1146, 1269, 1307, 1430, 3229, 3845
TS1	480i, 112, 232, 305, 334, 494, 879, 1097, 1321, 1599, 2183, 3142
	1021i, 100, 250, 330, 347, 566, 922, 1112, 1327, 1606, 2358, 3207
TS2	1301i, 105, 234, 287, 491, 616, 732, 862, 1044, 1465, 1696, 2558
	1458i, 112, 224, 391, 506, 656, 773, 882, 1111, 1483, 1738, 2528
TS3	1783i, 113, 283, 414, 529, 668, 813, 1071, 1211, 1262, 1838, 2953
	2852i, 108, 269, 435, 553, 728, 909, 1114, 1245, 1325, 1783, 3022
TS4	479i, 90, 227, 252, 395, 662, 1020, 1137, 1413, 1528, 2960, 3978
	519i, 129, 240, 448, 684, 863, 1095, 1153, 1304, 1348, 2921, 3040
TSi	1509i, 104, 279, 361, 462, 546, 788, 904, 1250, 1326, 2274, 3129
	1690i, 112, 293, 457, 496, 622, 825, 943, 1197, 1342, 2415, 3169

[a] Results of Ref. [12].

changes that clearly demonstrate the strengthening of C–O bonding. Similar structural changes are observed on going from FCH$_2$OCl to ClCH$_2$OCl (C–O distance from 1.425 to 1.388 Å and O–Cl distance from 1.729 to 1.742 Å at the B3LYP level).

The other three conformers, denoted as C_1, C_2 and C_3 originate from the rotation of the methylic Cl around the C–O bond. The configurations obtained are the *trans* structure with respect to the two chlorine atoms (C_1, energy minimum), the *cis* structure with respect to one hydrogen and the hypochlorite chlorine (C_2, energy maximum) and the *cis* structure with respect to the two chlorines (C_3, energy maximum). C_1 is located 2.6 kcal mol^{-1} higher than C_0 at the G2MP2 level and 2.3 kcal mol^{-1} at the CCSD(T) level while C_2, C_3 are placed 3.1, 3.6 and 8.1, 9.2 kcal mol^{-1}, respectively, higher than C_0 at the G2MP2 and CCSD(T) levels. We can see that the higher rotational barrier corresponds to the *cis* Cl–Cl structure due to the repulsions between the two voluminous chlorine atoms. Several geometrical changes accompany these conformations as a result of the various interactions between the chlorine atoms and the methylic hydrogens (Table 3). The C–O bond distance

increases in the order $C_0 < C_2 < C_1 < C_3$ while the O–Cl bond distance decreases in the order $C_0 \sim C_1 > C_2 > C_3$. The Cl–C distance is the same in C_0 and C_2 and decreases similarly in C_1 and C_3.

Dichloromethanol, Cl$_2$CHOH, the isomeric form of chloromethyl hypochlorite, is found to be more stable than ClCH$_2$OCl by 42.8 and 46.1 kcal mol^{-1} at the G2MP2 and CCSD(T)/6-311+G(d,p)//MP2/6-311+G(d,p) levels, respectively. The present results are in good agreement with the stabilization energies 43.7 [11] and 41.2 kcal mol^{-1} [15] reported in the literature. The structure of the isomerization transition state TSi results from the elongation of the O–Cl and C–H bonds (to 2.206, 2.081 and 1.383, 1.347 Å, respectively, at the B3LYP/6-311+G(d,p) and MP2/6-311+G(d,p) levels) with a simultaneous approach of the hypochlorite chlorine to the carbon atom. It is located considerably high at 53.6 and 56.8 kcal mol^{-1} above ClCH$_2$OCl at the G2MP2 and CCSD(T) levels, respectively, which may be considered comparable within the uncertainty limits of the methods and consistent with the value of ~ 52 kcal mol^{-1} reported by Mühlhäuser et al. [15]. The tensions originating from the triangular geometries involved in TSi explain the high barrier to isomerization. Thus, although dichloromethanol is thermodynamically much more stable than chloromethyl hypochlorite, the isomerization process (reaction (5)) is completely hindered at the thermal energy region by the high critical energy required.

The vibrational harmonic frequencies (Table 4) of the two minima are consistent in both sets of optimization and in accord with the literature results [12]. Some discrepancies are observed in the imaginary frequencies of the transition states, which may be related to the few differences obtained in the structural parameters among the two optimized geometries.

3.2. Elimination pathways

The various dissociation channels may be classified into the 1,1 and 1,2 eliminations and the C–O, O–Cl bond scissions.

The 1,1 eliminations (reactions (1) and (2)) may lead to either *cis*-HCOCl+HCl or to *cis*-ClCOCl+H$_2$ products through transition states TS1 and TS2, respectively. The corresponding structural parameters are depicted in Table 3 and Fig. 2 and they are generally consistent in both optimization procedures. The only exception is the C–Cl bond distance in TS1, which assumes a very elongated value, 2.516 Å in B3LYP, compared to the MP2 value, 2.175 Å. The associated barriers are quite high, 47.8, 73.0 kcal mol^{-1} at the G2MP2 level and 43.5, 71.7 kcal mol^{-1} at the CCSD(T) level above reactant. Also the products, *cis*-HCOCl+HCl and *cis*-ClCOCl+H$_2$, are more unstable than the reactant, located higher than ClCH$_2$OCl at 26.4 and 41.1 kcal mol^{-1}, respectively, at the G2MP2 level and at 21.2 and 30.4 kcal mol^{-1} at the CCSD(T) level. Thus, the 1,1 eliminations are not probable

ClCH₂OCl
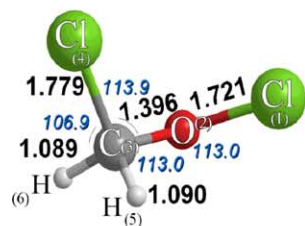
Cl(1)-O(2)-C(3)-Cl(4) = 72.6
Cl(1)-O(2)-C(3)-H(5) = - 49.3
Cl(1)-O(2)-C(3)-H(6) = - 170.4
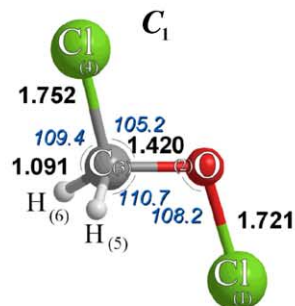
Cl(1)-O(2)-C(3)-Cl(4) = 180.0
Cl(1)-O(2)-C(3)-H(5) = 62.0
Cl(1)-O(2)-C(3)-H(6) = - 62.0
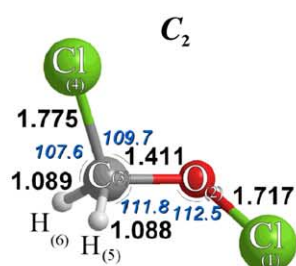
Cl(1)-O(2)-C(3)-Cl(4) = 118.7
Cl(1)-O(2)-C(3)-H(5) = 0.0
Cl(1)-O(2)-C(3)-H(6) = - 124.3
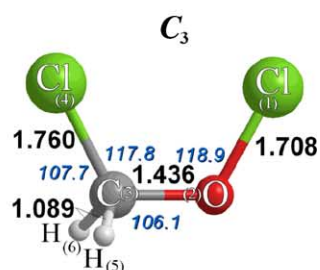
Cl(1)-O(2)-C(3)-Cl(4) = 0.0
Cl(1)-O(2)-C(3)-H(5) = - 120.6
Cl(1)-O(2)-C(3)-H(6) = 120.6
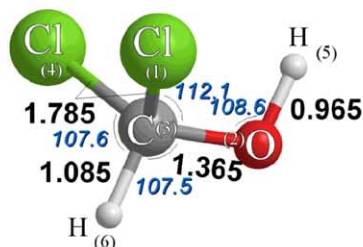
H(5)-O(2)-C(3)-Cl(1) = - 61.9
H(5)-O(2)-C(3)-Cl(4) = 61.9
H(5)-O(2)-C(3)- H(6) = 180.0

CHCl₂OH

Fig. 1. Optimized structures of conformers and isomers of ClCH₂OCl at the MP2/6-311 + G(d,p) level of theory.

decomposition pathways in the thermal region and may gain significance only under photoactivation of ClCH₂OCl.

The 1,2 eliminations (reactions (3) and (4)) lead to HCClO + HCl or to HCHO + Cl₂ products, which are thermodynamically more stable than ClCH₂OCl. In particular, chlorinated formaldehyde and HCl are the most stable products at all levels of theory, located at 44.6 kcal mol⁻¹ at the G2MP2 level and 50.4 kcal mol⁻¹ at the CCSD(T) level below reactant. Plain formaldehyde and Cl₂ are also located below ClCH₂OCl at 3.1

and 3.0 kcal mol⁻¹ at the G2MP2 and CCSD(T) levels, respectively. The corresponding transition states, TS3 and TS4, both present rectangular geometries and are formed by the elongation of the O–Cl, C–H bonds (reaction (3)) and the O–Cl, C–Cl bonds (reaction (4)). The calculated structural parameters are generally in agreement between the two methods with a discrepancy, only observed in the optimized TS4 structures where the elongation of the C–Cl bond is predicted to be quite large in the B3LYP method, 2.293 Å, compared to the MP2 value, 1.909 Å. However,
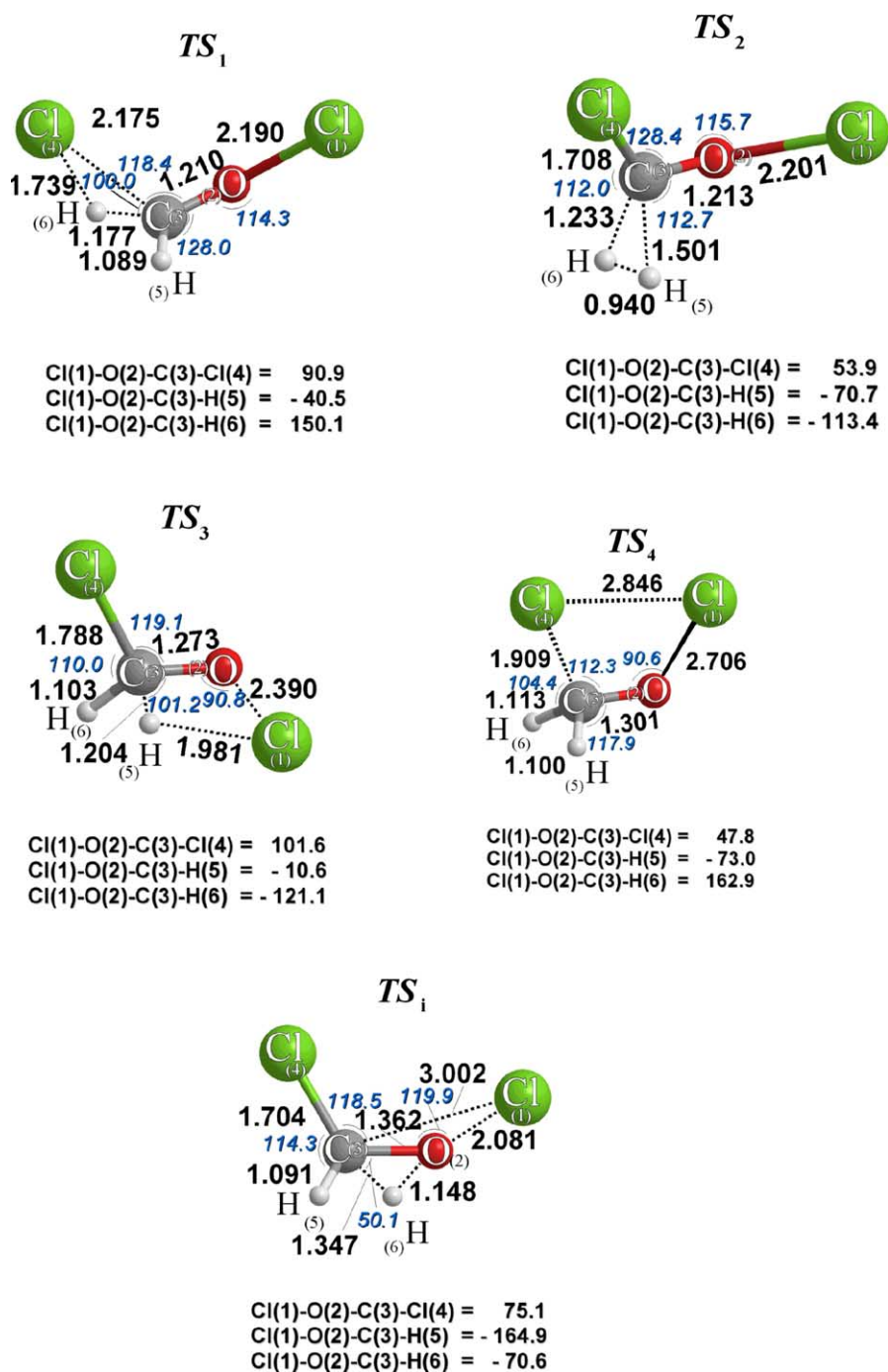
Fig. 2. Optimized structures for transition state configurations of various decomposition and isomerization channels of CH$_2$ClOCl at the MP2/6-311+G(d,p) level of theory.

the remaining parameters and the vibrational frequencies are consistent in both optimizations. Although, the products in the 1,2 eliminations are more stable than the reactant ClCH$_2$OCl, the intervening barriers corresponding to TS3 and TS4 are again quite high as in the 1,1 eliminations. Also, some differences from the G2MP2 to CCSD(T)/6-311+G(d,p)//B3LYP/6-311+G(d,p) results are observed (Table 5). Thus, TS3 is located at 64.3 and 43.5 kcal mol^{-1} above reactant and TS4 at 50.3 and 38.0 kcal mol^{-1} at

the G2MP2 level and CCSD(T) levels, respectively. Apart from these deviations however, both methods predict that the most probable 1,2 elimination is the production of HCHO+Cl$_2$. This channel presents the lowest critical energy for reaction among all dissociation pathways at the CCSD(T) level. The G2MP2 method predicts that the lowest critical energy channel is the formation of *cis*-HCOCl+ HCl. Given the fact though, that the difference of ∼2.5 kcal mol^{-1} between the critical energies of reactions

Table 5
Relative energy results (including ZPE corrections) in kcal mol^{-1} for ClCH$_2$OCl decomposition and isomerization channels

Species	B3LYP/ 6-311+ G(d,p)	MP2/ 6-311+ G(d,p)	G2MP2	CCSD(T)/ 6-311+ G(d,p)
ClCH$_2$OCl	0.0	0.0	0.0	0.0
TS1	34.3	48.6	47.8	43.4
cis-HCOCl+HCl	18.2	20.5	26.4	21.2
TS2	65.4	72.1	73.0	71.7
cis-ClCOCl+H$_2$	32.2	28.3	41.1	30.4
TS3	44.9	52.4	64.3	43.5
ClCHO+HCl	−50.4	−53.0	−44.6	−50.4
TS4	47.0	50.5	50.3	38.0
HCHO+Cl$_2$	−6.1	−1.9	−3.1	−3.0
TSi	48.4	52.5	56.8	53.6
Cl$_2$CHOH	−43.3	−49.2	−42.8	−46.1
ClCH$_2$+OCl	68.5	84.6	78.7	73.7
ClCH$_2$O+Cl	48.4	42.8	49.7	36.2

(1) and (4) is within the uncertainty limits of the methodology and taking into account the high instability of the products of reaction (1), we may conclude that the main decomposition channel predicted by G2MP2 is also the formation of HCHO+Cl$_2$.

To summarize, the critical energy order of the various decomposition and isomerization pathways according to G2MP2 methodology is TS1∼TS4<TSi<TS3<TS2. According to the CCSD(T) method, the corresponding order is TS4<TS1∼TS3<TSi<TS2. TS2 is very high located in both G2MP2 and CCSD(T), well separated from the other critical energy barriers, TS1, TS3, TS4 and TSi, which may be considered to be closely spaced within the uncertainty limits of the quantum mechanical techniques employed. Consideration of the thermodynamic stability of the products indicates that the dominant decomposition pathways are the 1,2 eliminations followed by the isomerization to dichloromethanol.

3.3. Bond fission processes.

Reactions (6) and (7) represent the breaking of the O–Cl and C–O bonds. The fission products, chloromethoxy
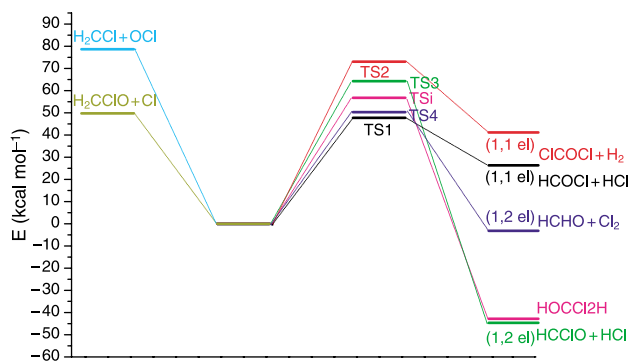
Fig. 3. Energy profile for CH$_2$ClOCl unimolecular decomposition and isomerization at the G2MP2 level.
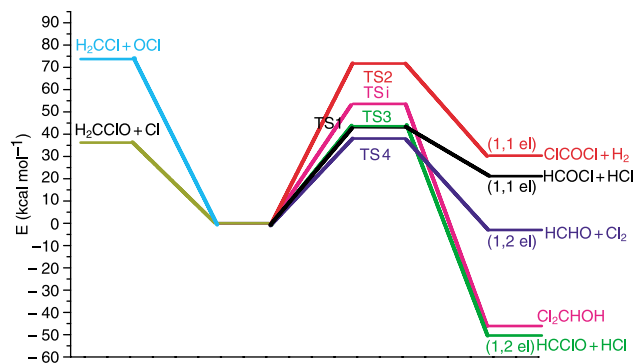
Fig. 4. Energy profile for CH$_2$ClOCl unimolecular decomposition and isomerization at the CCSD(T)/6-311+G(d,p)//B3LYP/6-311+G(d,p) level.

radical and chlorine atom or chloromethyl radical and chlorine monoxide are located at 49.7, 78.7 kcal mol^{-1} at the G2MP2 level and 36.2, 73.7 kcal mol^{-1} at the CCSD(T) level, respectively. These values also represent the critical energies required for the bond scission processes and at the same time the internal energy acquired by ClCH$_2$OCl in the reverse association reactions. Thus, chloromethyl hypochlorite formed in the association reaction of ClCH$_2$ and ClO, has enough energy to dissociate according to the decomposition channels examined or isomerize to dichloromethanole. If some internal energy loss does take place though, which is very probable under moderate pressure conditions (one atmosphere for instance) ClCH$_2$OCl is shown to present a remarkable stability at thermal energies and make a temporary reservoir species.

The critical energy for O–Cl bond breaking presents the lowest value among all decomposition channels at the CCSD(T) calculations and it is comparable with the 1,2 elimination pathway leading to HCHO+Cl$_2$. Indeed, photolytic Cl release is shown to be the most probable pathway, leading to chloromethoxy radical known to decompose through C–Cl bond scission [19,20]. Thus, HCHO is a major reaction product in ClCH$_2$OCl dissociation, formed either directly (reaction (4)) or indirectly through the CClH$_2$O intermediate.

3.4. Comparison with other hypochlorites

Comparison with the dissociation of simple methyl hypochlorite shows interesting correlations in the decomposition scheme. In the CH$_3$OCl system, the critical energies for the main pathways, i.e. the 1,2 HCl elimination and the isomerization channel are found to be 53.1 and 62.7 kcal mol^{-1}, respectively, at the G2MP2 level [10, 13]. The corresponding barriers in ClCH$_2$OCl are also quite high, 64.3 and 56.8 kcal mol^{-1} at the G2MP2 level but in the opposite order favouring isomerization. Another interesting feature is the same energy barrier required for the 1,1 H$_2$ elimination and for the breaking of the C–O bond. They are found to be ∼72 and ∼78 kcal mol^{-1},

respectively, at the G2MP2 level for both systems showing no particular influence of the substitution of a methylic hydrogen by a chlorine atom on the C–H and C–O bond energies. The comparison with FCH_2OCl shows other analogies. Here, we observe close isomerization barriers, 43.8 and 48.4 kcal mol^{-1} at the B3LYP level for FCH_2OCl and $ClCH_2OCl$, respectively, which, coupled with the observation mentioned above, point out to easier isomerization in the case of substituted methyl hypochlorites. In contrast, the 1,2 HCl elimination in FCH_2OCl presents a critical energy higher around 10 kcal mol^{-1} compared to $ClCH_2OCl$ at the B3LYP level.

From the above discussion, it is clear that all cases present high energy barriers to decomposition. Photoactivation appears to be the most probable means to reaction. We may thus, conclude that simple and halogenated methyl hypochlorites, once formed, are very stable species, able to act as temporary halogen reservoir species.

References

[1] M.J. Molina, F.S. Rowland, Nature 249 (1974) 810.
[2] J.N. Crowley, F. Helleis, R. Müller, G.K. Moortgat, P.J. Crutzen, J.J. Orlando, J. Geophys. Res. 99 (1994) 20683.
[3] J.N. Crowley, P. Campuzano-Jost, G.K. Moortgat, J. Phys. Chem. 100 (1996) 3601.
[4] S.A. Carl, C.M. Roehl, R. Müller, G.K. Moortgat, J.N. Crowley, J. Phys. Chem. 100 (1996) 17191.
[5] V. Daele, G. Laverdet, G. Poulet, Int. J. Chem. Kinet. 28 (1996) 589.
[6] B.M. Messer, M.J. Elrod, Chem. Phys. Lett. 301 (1999) 10.
[7] J.S. Francisco, Int. J. Quant. Chem. 73 (1999) 29.
[8] Y. Li, J.S. Francisco, J. Chem. Phys. 111 (1999) 8384.
[9] J. Espinoza-Garcia, Chem. Phys. Lett. 315 (1999) 239.
[10] J. Espinoza-Garcia, Chem. Phys. Lett. 316 (2000) 316.
[11] T.-J. He, D.-M. Chen, F.-C. Liu, L.-S. Sheng, Chem. Phys. Lett. 332 (2000) 545.
[12] D. Jung, C.-J. Chen, J.W. Bozzelli, J. Phys. Chem. A 104 (2000) 9581.
[13] D. Shah, C.E. Canosa-Mas, N.J. Hendy, M.J. Scott, A. Vipond, R.P. Wayne, PCCP 3 (2001) 4932.
[14] E. Drougas, A.M. Kosmas, M. Schnell, M. Mühlhäuser, S.D. Peyerimhoff, Mol. Phys. 100 (2002) 2653.
[15] M. Mühlhäuser, M. Schnell, S.D. Peyerimhoff, Mol. Phys. 100 (2002) 2719.
[16] E. Drougas, D.K. Papayannis, A.M. Kosmas, Chem. Phys. 276 (2002) 15.
[17] Z.Y. Zhou, X.L. Cheng, H. Fu, X.M. Zhou, Struct. Chem. 15 (2004) 185.
[18] M.J. Frisch, G.W. Trucks, H.B. Schlegel, G.E. Scuseria, M.A. Robb, J.R. Cheeseman, V.G. Zakrzewski, J.A. Montgomery, Jr., R.E.Stratmann, J.C. Burant, S. Dapprich, J.M. Millam, A.D. Daniels, K.N. Kudin, M.C. Strain, O. Farkas, J. Tomasi, V. Barone, M. Cossi, R. Cammi, B. Mennucci, C. Pomelli, C. Adamo, S. Clifford, J. Ochterski, G.A. Petersson, P.Y. Ayala, Q. Cui, K. Morokuma, D.K. Malick, A.D. Rabuck, K. Raghavachari, J.B. Foresman, J. Cioslowski, J.V. Ortiz, B.B. Stefanov, G. Liu, A. Liashenko, P. Piskorz, I.. Komaromi, R. Gomperts, R.L. Martin, D.J. Fox, T. Keith, M.A. Al-Laham, C.Y. Peng, A. Nanayakkara, C. Gonzalez, M. Challacombe, P.M.W. Gill, B.G. Johnson, W. Chen, M.W. Wong, J.L. Andres, C.M. Head-Gordon, E.S. Replogle, J.A. Pople, GAUSSIAN 98, Revision A.9, Gaussian Inc., Pittsburgh, PA, (1998).
[19] H. Hou, B. Wang, Y. Gu, J. Phys. Chem. A 103 (1999) 8075.
[20] F. Wu, R.W. Carr, J. Phys. Chem. A 106 (2002) 5832.